analytical chemistry



pubs.acs.org/ac
Article

# Analysis of Carbon Materials with Infrared Photoacoustic Spectroscopy

Ton-Rong Tseng,* Che-Hua Yang,* Hsiao-Chi Lu, Ching-Ping Liu, and Bing-Ming Cheng*

Cite This: *Anal. Chem.* 2024, 96, 10732−10737
Read Online

ACCESS | Metrics & More | Article Recommendations | Supporting Information

**ABSTRACT:** Measurement of infrared spectroscopy has emerged as a significant challenge for carbon materials due to the sampling problem. To overcome this issue, in this work, we performed measurements of IR spectra for carbon materials including $C_{60}$, $C_{70}$, diamond powders, graphene, and carbon nanotubes (CNTs) using the photoacoustic spectroscopy (PAS) technique; for comparison, the vibrational patterns of these materials were also studied with a conventional transmission method, diffuse reflectance infrared Fourier transform (DRIFT) spectroscopy, or Raman spectroscopy. We found that the IR photoacoustic spectroscopy (IR-PAS) scheme worked successfully for these carbon materials, offering advantages in sampling. Interestingly, the profiles of IR-PAS spectra for graphene and CNTs exhibit negative bands using carbon black as the reference; the negative spectral information may provide valuable knowledge about the storage energy, production, structure, defect, or impurity of graphene and CNTs. Thus, this approach may open a new avenue for analyzing carbon materials.

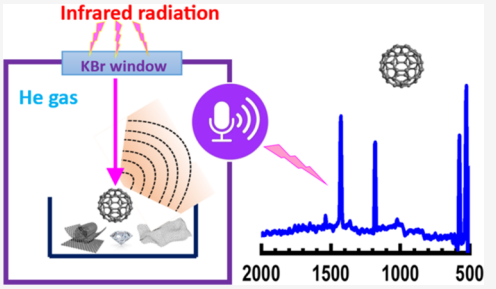




## INTRODUCTION

Photoacoustic spectroscopy is an unusual form of spectroscopy, frequently referred to by the acronym PAS,[1−7] which consists of a spectrum of the intensity of the acoustic signal detected by a microphone or a piezoelectric detector, against the excitation wavelength or photon energy. In short, PAS measures the response of light on a sample through acoustic detection. Using this means, the absorbed light generates heat in a sample, creating thermal expansion and eventually producing a pressure wave or sound that is monitored in the form of an acoustic wave detected by a piezoelectric sensor or a microphone.

Combined with an infrared source, IR photoacoustic spectroscopy (IR-PAS) was developed in 1968.[8−14] Using modern equipment and light sources, IR-PAS analyzes materials with several advantages including minimal sample preparation, being suitable for opaque materials, and being nondestructive for analytes. The IR-PAS technique thus proves attractive to researchers to expand its unique spectroscopic property for analysis of materials; furthermore, the scientific community is exploring new applications of this technique for various forms of samples, including gaseous molecules, liquids, solids, and powders.[6,15−19]

Materials containing elemental carbon with a very high ratio (above 80%) can be classified as carbon materials; these may include graphenes, graphites, diamonds, fullerenes, chars, shoots, cokes, and carbonaceous solids. Sometimes, analysis of these carbon materials might be difficult or even impossible by using transmission techniques; indeed, measuring the infrared absorption spectra of these carbon materials poses significant challenges due to sampling issues. Instead, we believe that the PAS technique may successfully enable the acquisition of the IR spectra for carbon materials while eliminating these difficulties;[20−29] therefore, it is worthwhile to pay particular attention to the analysis of carbon materials using the IR-PAS technique.

Considering that the IR-PAS scheme may be useful and feasible to study carbon materials, we performed measurements of IR spectra using the PAS procedure for materials including $C_{60}$, $C_{70}$, graphene, carbon nanotubes (CNTs), and diamond powders. We also compared their IR spectra measured by the PAS technique with other spectroscopic methods in this work.

## EXPERIMENTAL SECTION

The spectra of the carbon materials were measured with an IR-PAS system, in which the PAS accessory attached to a microphone detector (model number PAC300) was provided by MTEC Photoacoustic, Inc. This PAS part was coupled to a Fourier transform infrared (FTIR) spectrometer (ABB FTLA2000-104, Quebec, Canada).[30] To reduce interference from environmental gases, the FTIR spectrometer was flushed out with gaseous nitrogen. Meanwhile, the PAS cell was purged with helium gas to enhance the sensitivity of the signal; by this

Received: April 6, 2024
Revised: May 20, 2024
Accepted: June 4, 2024
Published: June 14, 2024

means, the flow rate of He was regulated below 5 cc/s to avoid blowing sample powders into the detector. The samples were placed in a stainless-steel cup, provided by MTEC Photoacoustic Inc., with part number LSC001. We lifted up the sampling cup in the gaseous He environment under atmospheric pressure; usually, the samples were loaded into the cup at depths of about 2 mm. As a reference, the carbon black disk was also supplied by MTEC Photoacoustic Inc. with part number SH008. Typically, we recorded 512 scans for the IR-PAS spectra with a resolution of 8 $cm^{-1}$.

For comparison, the spectra of carbon materials were also measured by using other techniques. For the infrared absorption spectra obtained by the transmission mode, the samples were recorded with the interferometric spectrometer ABB FTLA2000-104 or the Nicolet Magna 860, in which a KBr beamsplitter and a HgCdTe or DTGS detector were used to span the mid-infrared range of 4000−500 or 4000−400 $cm^{-1}$, respectively. The FTIR spectrometer was also purged with gaseous nitrogen during the measurements. The absorption spectra were typically collected with 512 scans and with a resolution of 1 $cm^{-1}$.

For the Raman shift spectrum, a Raman spectrometer, Micro Raman Identification (MRI), provided by Pro Trust Tech Co. Ltd., equipped with a charge coupled device (CCD) detector was used in the measurement., wherein the light at 532 nm was used to excite the samples with a beam size of 1.1 × 2.2 $mm^2$.[31] The Raman shift spectrum could be scanned in the range of 186−3500 $cm^{-1}$ with a resolution of 1.8 $cm^{-1}$. As the powder samples might be unevenly distributed on the substrate, the Raman shift spectra thus suffered from distortion of the baselines. Selection of the position monitored could enable the distortion to be minimized.

IR spectra of diamond powders were also recorded with a diffuse reflectance accessory (Spectra-Tech) attached to the FTIR spectrometer (Bomem DA8), for which a KBr beamsplitter and a HgCdTe detector were used.[32] The FTIR was operated in vacuum mode to eliminate the absorption of environmental water vapor and carbon dioxide from the spectra. For the measurement of the diffuse reflectance infrared Fourier transform (DRIFT) spectrum, KBr powder was used as a reference. Typical spectra were measured with a resolution of 1 $cm^{-1}$ and 200 scans.

Materials of $C_{60}$ (99.95%), $C_{70}$ (98%, up to 2% carbonaceous materials), carbon nanotube (multiwalled >95%; OD: 20−40 nm; L: 5−15 $\mu$m), and graphene (nanopowder 8 nm flakes) were purchased from UNI-ONWARD Corp.; however, the natural diamond powder of size 10 $\mu$m was purchased from WEC Superabrasives. For the absorption measurement, thin films of $C_{60}$ and $C_{70}$ were prepared on the KBr window; for this purpose, a saturated solution of $C_{60}$ and $C_{70}$ in xylene solvent was slowly sprayed onto a KBr window that was placed on top of a heater. Then, the substrates with the films of $C_{60}$ and $C_{70}$ were placed in a vacuum oven at 150 °C for 24 h. For the PAS measurements, the samples were placed directly in the LSC001 cup without any pretreatment.

## RESULTS AND DISCUSSION

**Carbon Black as a Reference for IR-PAS.** Usually, IR-PAS uses signals from carbon black as a reference. Hence, we measured the PAS-responsive curve of the carbon black sample (provided by MTEC PAC300 with part number SH008) in a single-beam mode first; as the reference, Figure 1(a) depicts this raw curve in the mid-IR region 4000−500 $cm^{-1}$. The

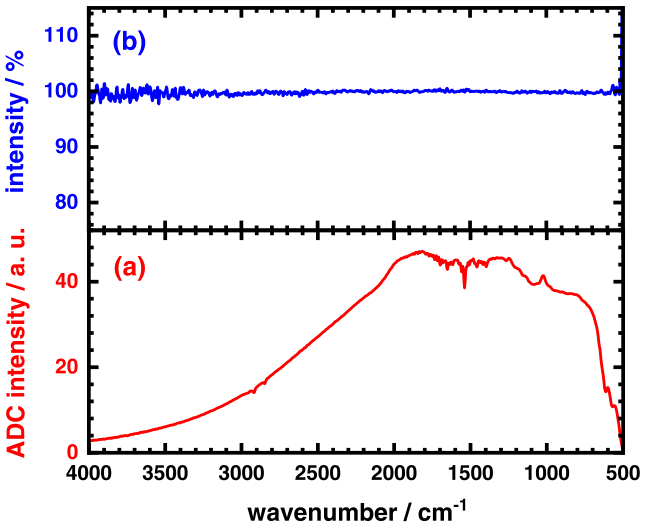


**Figure 1.** IR photoacoustic spectra of the carbon black (provided by MTEC PAC300 with part number SH008) in the wavenumber region 4000−500 $cm^{-1}$: (a) spectrum from a single-beam mode and treated as a reference, and (b) ratio spectrum (in percentage scale) of the two curves recorded consecutively in 15 min.

profile of this IR-PAS curve of carbon black reveals overlapping of the weak absorption of gaseous water in the wavenumber region 1700−1300 $cm^{-1}$ but no signal from the environmental carbon dioxide near 2350 $cm^{-1}$. The air did contain the vapor of water and environmental carbon dioxide, as could be observed in the background of the IR spectrum without any pretreatment. In this work, we purged the optical path of the IR instrument with high-purity nitrogen gas and the sampling cell with high-purity helium gas; by this means, we could remove any detectable carbon dioxide. However, the purging gases might introduce impurities in water, or the entire instrumental system might release gaseous water from the surface; as a result, we could still observe the weak signal of gaseous water in the spectrum.

To test the performance of the IR-PAS spectrometer, we subsequently recorded the next scan for the same carbon black sample 15 min later. Accordingly, Figure 1(b) displays the ratio spectrum from the two curves obtained consecutively for the same carbon black in the percentage scale; undoubtedly, this IR-PAS ratio spectrum is almost linear without perturbation from environmental moisture. The noise for peak-to-peak variation was well below 0.5% in the wavenumber region 3000−600 $cm^{-1}$. The result demonstrated that this IR-PAS system operated under stable conditions with good sensitivity.

**IR-PAS of Fullerenes.** To measure the IR-PAS spectra of the powders for carbon materials, we can directly place the powders in the sample cup and record their PAS curves; subsequently, the raw curves of the samples were divided by the reference spectrum of the carbon black, as shown in Figure 1(a), resulting in the final IR-PAS spectra. By this means, the IR-PAS spectrum of the $C_{60}$ powders obtained is displayed in Figure 2(a); accordingly, the intramolecular vibrational bands of IR-PAS for $C_{60}$ powders were clearly observed at 525, 575, 1182, 1429, and 1539 $cm^{-1}$. For comparison, we also measured the absorption spectrum of the $C_{60}$ film with the transmission method, in which the film was prepared by dropping the saturated $C_{60}$ solution, in xylene, onto a KBr window and was then dried in a vacuum oven at 150 °C overnight. The


https://doi.org/10.1021/acs.analchem.4c01797
Anal. Chem. 2024, 96, 10732−10737

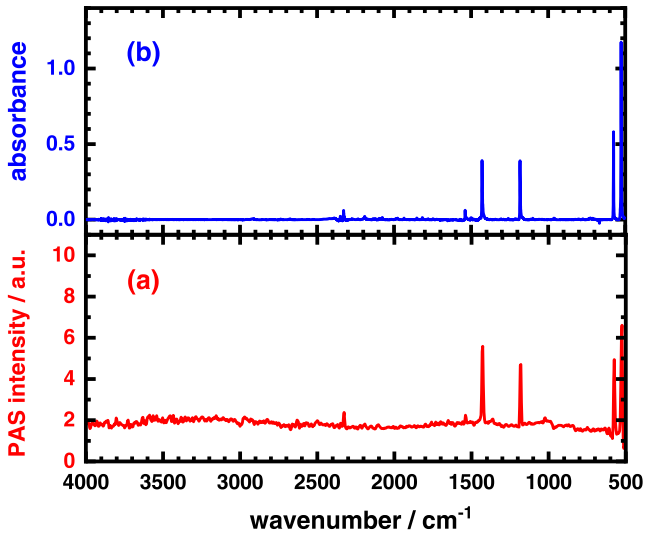


**Figure 2.** IR spectra of $C_{60}$ in the region 4000−500 $cm^{-1}$ at 300 K: (a) PAS spectrum of the powders (resolution 8 $cm^{-1}$) and (b) absorption spectrum of the film (resolution 1 $cm^{-1}$).

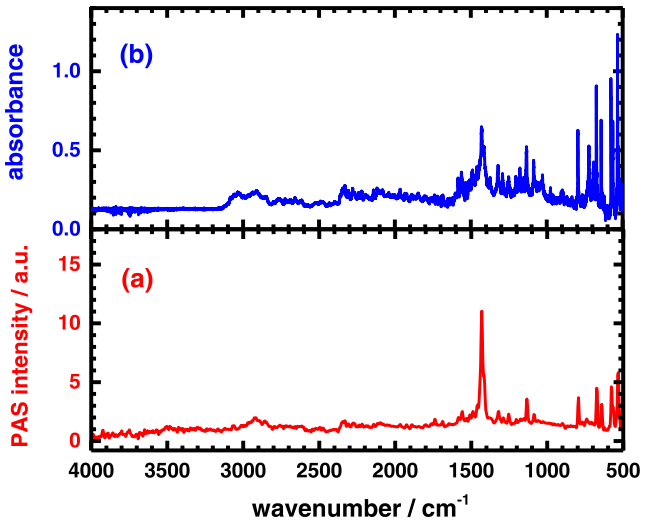


**Figure 3.** IR spectra of $C_{70}$ in the region 4000−500 $cm^{-1}$ at 300 K: (a) PAS spectrum of the powders (resolution 8 $cm^{-1}$) and (b) absorption spectrum of the film (resolution 1 $cm^{-1}$).

absorption spectrum of the $C_{60}$ film shown in Figure 2(b) displays the absorption bands of the $C_{60}$ film for infrared-active intramolecular vibrational modes at 527, 576, 1183, and 1429 $cm^{-1}$ corresponding to $F_{1u}(1)$, $F_{1u}(2)$, $F_{1u}(3)$, and $F_{1u}(4)$ with $F_{1u}$ symmetry and at 1539 $cm^{-1}$ corresponding to the $F_{1g}(2)$ + $H_u(2)$ group.[33−41] Comparing Figure 2(a,b), the positions of bands of IR-PAS recorded from $C_{60}$ powders and those of absorption obtained from the $C_{60}$ film are in satisfactory agreement, as listed in Table S1 (see in the Supporting Information). Overall, both spectral profiles look very similar in shape.

The fullerene consisting of 70 carbon atoms is $C_{70}$, which is made of 25 hexagons and 12 pentagons with a $D_{5h}$ symmetry; its structure is similar to that of the $C_{60}$ molecule, having 20 hexagons and 12 pentagons, with an $I_h$ symmetry. Readily, the IR spectrum of the $C_{70}$ powders determined by the PAS method and that of the $C_{70}$ film measured by the absorption technique are shown in Figure 3(a,b), respectively; similarly, the sampling procedures of the powders and the film for $C_{70}$ samples were the same as those for $C_{60}$ samples. Likewise, the positions of the IR bands of the $C_{70}$ sample examined by the PAS technique for the powders and those scanned by the absorption method for the film appear to be in good agreement, as listed in Table S2 (see in the Supporting Information);[33,41−45] however, the profile of PAS for the powders and that of absorption for the film exhibit a slight difference. The strongest IR band of the $C_{70}$ powders is at 1431 $cm^{-1}$ in the PAS spectrum, whereas that of the film is at 534 $cm^{-1}$ in the absorption spectrum. PAS is an indirect absorption spectroscopy technique; here, the ground-state molecule is excited to a higher energy state after absorbing light energy and returns to the ground state by nonradiative transition with the release of heat. Thus, the intensity of the PAS is proportional to the absorption coefficient ($\alpha$) and the conversion efficiency ($\eta$) of the absorbed light energy into heat. On comparison of the absorption and PAS spectra in Figure 3, we may conclude that the conversion efficiencies are not constant in the IR region for $C_{70}$.

Overall, the IR spectra of fullerenes $C_{60}$ and $C_{70}$ could be successfully measured by the PAS technique. Compared with the transmission method, the positions of the bands in PAS for the powder agree very well with those in absorption for the film, but the spectral profiles might differ in both techniques. Exclusively, the IR-PAS measurement has an advantage in sampling for fullerenes; with this benefit, the fullerene samples could be directly applied to measurements without any further treatment in the IR-PAS technique.

**IR-PAS of Diamond Powders.** Natural diamonds are rarely pure and may be contaminated with hydrogen, boron, nitrogen, and other elements. The impurities and defects in diamonds can be distinguished by their infrared spectra.[32,46−54] For the analysis of contaminants and color centers in powdered diamonds, we might try to use IR-PAS to avoid further sample preparation. The characteristic IR-PAS spectrum of natural diamond powder with size 10 $\mu$m was thus recorded, as shown in Figure 4(a); for comparison, the same sample was also measured by the diffuse reflectance infrared Fourier transform (DRIFT) technique, as displayed in Figure 4(b).

Twenty-one bands could be clearly detected from both spectra for the 10 $\mu$m natural diamond powders, as listed in Table S3 (see the Supporting Information). Here, four characteristic bands were recorded at 2933, 2964, 3107, and 3237 $cm^{-1}$ attributed to hydrogen impurities in the left part.[32,49,50,53,55] However, the strong absorption bands appearing in the central region at 1976, 2030, 2094, 2158, 2177, 2442, and 2515 $cm^{-1}$ are related to the intrinsic absorptions of two- and three-phonon processes for diamond itself.[32,51] In the fingerprint region, the prominent features are observed at 1282 and 1177 $cm^{-1}$, associated with an A (N2) center and a B (N4) center of a nitrogen defect. Additionally, the small shoulder at 1096 $cm^{-1}$ is induced by the A center, while the other small bands at 737, 1011, and 1330 $cm^{-1}$ are induced by the B center. Another small peak at 1432 $cm^{-1}$ may be associated with the N3 center, and the weak band at 1368 $cm^{-1}$ is from platelets.[32,49−51,53,56−58] According to the spectra from Figure 4(a,b), this natural diamond powder thus belongs to the type IaAB.

Diamond is the hardest natural material and cannot be dissolved intact in any solvent, which complicates sample preparation for transmission IR spectra. Instead, powdered


https://doi.org/10.1021/acs.analchem.4c01797
Anal. Chem. 2024, 96, 10732−10737

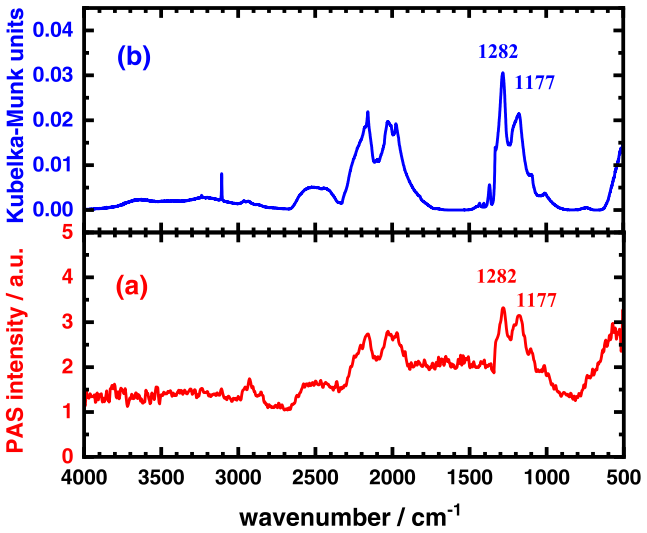


**Figure 4.** IR spectra of natural diamond powders with size 10 $\mu$m in the region 4000−500 $cm^{-1}$ at 300 K: (a) PAS spectrum (resolution 8 $cm^{-1}$) and (b) diffuse reflectance IR spectrum (resolution 1 $cm^{-1}$). The lines at 1282 and 1177 $cm^{-1}$ are marked and associated with A (N2) and B (N4) centers, respectively, due to nitrogen defects in diamond; this diamond accordingly belongs to the type IaAB.

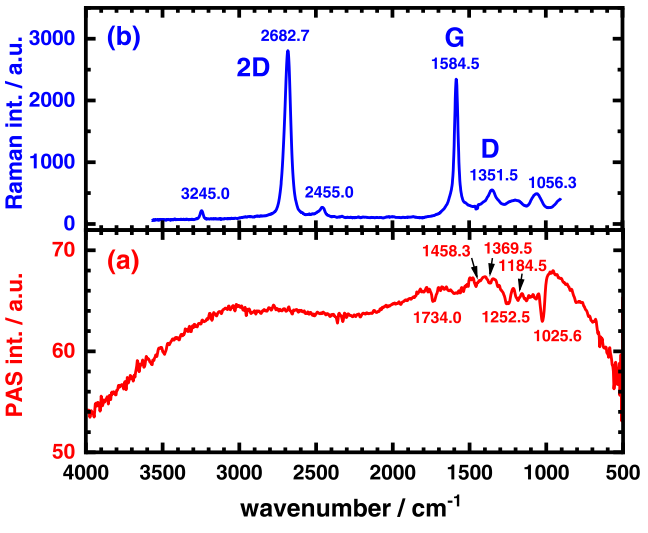


**Figure 5.** Spectra of graphene at 300 K: (a) IR-PAS spectrum and (b) Raman shift spectrum excited at 532 nm.

diamonds may be directly analyzed using the IR-PAS or DRIFT technique without further sampling. As a demonstration, both techniques can successfully obtain IR spectra for diamond powders. Although both spectra show similarity in profiles, the intensity of the IR spectrum from the DRIFT technique is higher than that from the PAS method for diamond powders. Thus, we might conclude that the former technique is more sensitive for identifying the type of diamond powders.

**IR-PAS of Graphene.** Graphene, one of the allotropes of carbon, is a material that has a single layer of carbon atoms with a thickness of only 335 pm. Rediscovered, isolated, and investigated in 2004,[59] graphene and its characteristic spectra have since been extensively studied using various spectroscopic techniques. In this work, graphene samples were measured with the IR-PAS and Raman techniques at approximately 300 K as displayed in Figure 5(a,b), respectively, for comparison. Graphene consists of a single layer of atoms arranged in a hexagonal lattice nanostructure; as a result, each carbon is connected to its three nearest neighbors by an $sp^2$ bond. Raman spectroscopy is sensitive to symmetric covalent bonds; thus, it can provide a wealth of information about the structure of graphene.[60−62] The unique Raman shift spectrum of the graphene sample is revealed in Figure 5(b), where the characteristic D, G, and 2D peaks of graphene were clearly identified at 1351.5, 1584.5, and 2682.7 $cm^{-1}$, respectively. The D band is associated with $sp^3$ hybridized carbon atoms and defects within the carbon atom plane, while the G band is associated with the pristine lattice of $sp^2$ bonded carbon atoms in the graphene sheet. The D band (denoting disorder-induced) is known as the disorder band or the defect band; the intensity of the D band is directly proportional to the level of defects or impurities in the sample. The Raman spectrum in Figure 5(b) shows a noticeable D band, suggesting that this graphene sample contains defects or impurities, which may be characterized in the IR-PAS spectrum as shown in Figure 5(a).

Although the D, G, and 2D bands of graphene are active in the Raman spectrum, these bands are inactive in the IR spectrum as shown in Figure 5(a). However, the IR-PAS spectrum of graphene reveals other negative peaks but not positive ones, as displayed in Figures 2(a) and 3(a). It is not clear what the negative bands represent. The result might indicate that graphene may preserve the excitation energy of IR light instead of relaxing the energy by acoustic waves through these bands.

For preparation, it is difficult to synthesize graphene without defects or impurities. As shown in Figure 5(a), negative bands were observed at 1734.0, 1458.3, 1369.5, 1252.5, 1184.5, 1129.5, 1067.4, and 1025.6 $cm^{-1}$, which are associated with the vibrational bands of impurities or defects, including possible graphane, hydrogenated graphene, graphene oxides (GOs), or reduced-graphene oxides (rGOs) in graphene.[63,64]

Synthetic techniques like liquid-phase oxidation, gaseous phase etching, and templated growth have been employed to produce scalable graphenes. These methods might utilize GO, rGO, or other materials mentioned above as starting materials.[65−68] Thus, measuring the IR-PAS of graphene can provide valuable information on its production process and impurities within it; for this reason, a systematic investigation of IR-PAS on various types of graphenes needs to be conducted.

**IR-PAS of CNT.** The structure of the carbon nanotube (CNT) can be considered as a rolled-up graphene sheet around a core tube. Multiwalled carbon nanotubes (MWCNTs) may have many layers of graphene wrapped around the core tube. Similar to the spectra of graphene, the IR-PAS and Raman spectra of MWCNTs with diameter 20−40 nm were also measured close to 300 K in this work; the results of the former and the latter are displayed in Figure 6(a,b), respectively, for comparison. In the Raman shift spectrum of MWCNTs, the D, G, and 2D bands were recorded at 1342.4, 1576.6, and 2679.7 $cm^{-1}$, respectively;[69−71] these positions are close to those in graphene. Particularly, the more prominent D band in the MWCNT indicates more disorder in its structure.

Interestingly, the IR-PAS spectrum of MWCNT also possesses negative bands, similar to the one of graphene; meanwhile, the positions of these bands were recorded at the same values in both IR-PAS spectra. Thus, we expect that the IR-PAS of MWCNT might also provide valuable spectral information on the structure and functional groups of the


https://doi.org/10.1021/acs.analchem.4c01797
Anal. Chem. 2024, 96, 10732−10737

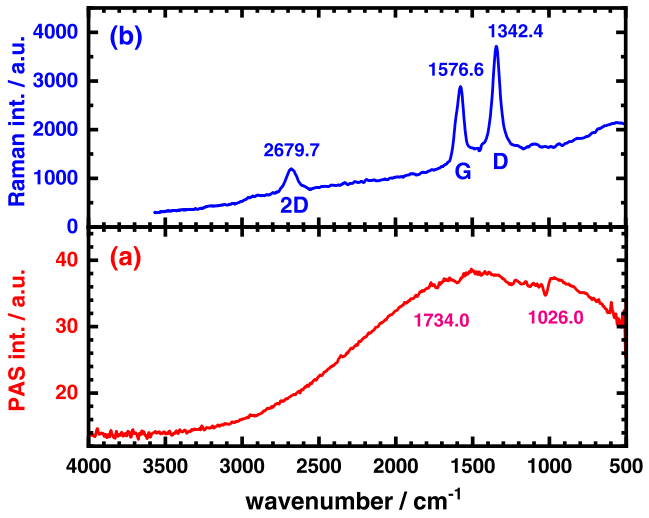


**Figure 6.** Spectra of multiwalled carbon nanotubes with diameter 20−40 nm at 300 K: (a) the IR-PAS spectrum and (b) the Raman shift spectrum excited at 532 nm.

CNT, related to its production, impurities, and properties. In the future, more work will still need to be conducted to thoroughly investigate the understanding and application of IR-PAS for CNTs.

## CONCLUSIONS

In this work, we performed the measurements of IR spectra on various carbon-related materials, like $C_{60}$, $C_{70}$, graphene, carbon nanotube, and diamond powders by using the photoacoustic spectroscopic technique. For comparison, the vibrational patterns of these materials were also examined by other spectral techniques including the transmission method, the diffuse reflectance infrared Fourier transform technique, or the Raman spectroscopic scheme. As a result, we conclude that the IR-PAS technique can successfully obtain valuable vibrational information on $C_{60}$, $C_{70}$, diamond powders, graphene, and CNT without sampling problems. Particularly, the IR spectra of PAS for graphene and CNT exhibit negative bands when using carbon black as the reference; these negative bands may provide valuable insights into storage energy, production, structure, defects, or impurities of these materials. Hence, this study may open a new avenue for analyzing carbon materials. For a full understanding and application of the IR-PAS, further studies need to be thoroughly conducted on these carbon materials in the future.

## ASSOCIATED CONTENT

### Data Availability Statement

All data discussed in the paper will be made available to readers on request to the corresponding author.

### Supporting Information

The Supporting Information is available free of charge at https://pubs.acs.org/doi/10.1021/acs.analchem.4c01797.

Positions and assignments of IR bands of $C_{60}$, $C_{70}$, and diamond powders (PDF)

## AUTHOR INFORMATION


### Corresponding Authors

**Ton-Rong Tseng** − *College of Mechanical and Electrical Engineering, National Taipei University of Technology, Taipei 10608, Taiwan*; Email: wellsimon@gmail.com

**Che-Hua Yang** − *College of Mechanical and Electrical Engineering, National Taipei University of Technology, Taipei 10608, Taiwan*; Email: chyang@ntut.edu.tw

**Bing-Ming Cheng** − *Department of Medical Research, Hualien Tzu Chi Hospital, Buddhist Tzu Chi Medical Foundation, Hualien City 970, Taiwan; Tzu-Chi University of Science and Technology, Hualien City 970, Taiwan*; orcid.org/0000-0002-8540-6274; Email: bmcheng7323@gmail.com

### Authors

**Hsiao-Chi Lu** − *Department of Medical Research, Hualien Tzu Chi Hospital, Buddhist Tzu Chi Medical Foundation, Hualien City 970, Taiwan*; orcid.org/0000-0002-0280-1317

**Ching-Ping Liu** − *Department of Chemistry, Fu Jen Catholic University, New Taipei City 242062, Taiwan*; orcid.org/0000-0003-3510-8583

Complete contact information is available at: https://pubs.acs.org/10.1021/acs.analchem.4c01797


### Notes

The authors declare no competing financial interest.

## ACKNOWLEDGMENTS

This work was supported by the National Science and Technology Council of Taiwan with Grant No. NSTC-112-2113-M-303-001.

## REFERENCES


(1) McClelland, J. F. *Anal. Chem.* **1983**, *55*, 89A−105A.
(2) West, G. A.; Barrett, J. J.; Siebert, D. R.; Reddy, K. V. *Rev. Sci. Instrum.* **1983**, *54*, 797−817.
(3) Haisch, C. *Meas. Sci. Technol.* **2012**, *23*, No. 012001.
(4) Patel, P.; Hardik, M.; Patel, P. *Int. J. Pharm. Erud.* **2013**, *3*, 41−56.
(5) Bekiaris, G.; Bruun, S.; Peltre, C.; Houot, S.; Jensen, L. S. *Waste Manage.* **2015**, *39*, 45−56.
(6) Yang, T.; Chen, W.; Wang, P. *Appl. Spectrosc. Rev.* **2021**, *56*, 143−170.
(7) Fathy, A.; Sabry, Y. M.; Hunter, I. W.; Khalil, D.; Bourouina, T. *Laser Photonics Rev.* **2022**, *16*, No. 2100556.
(8) Kerr, E. L.; Atwood, J. G. *Appl. Opt.* **1968**, *7*, 915−921.
(9) Kreuzer, L. B. *J. Appl. Phys.* **1971**, *42*, 2934−2943.
(10) Max, E.; Rosengren, L. G. *Opt. Commun.* **1974**, *11*, 422−426.
(11) Nordal, P. E.; Kanstad, S. O. *Opt. Commun.* **1977**, *22*, 185−189.
(12) Busse, G.; Bullemer, B. *Infrared Phys.* **1978**, *18*, 631−634.
(13) Rockley, M. G.; Devlin, J. P. *Appl. Spectrosc.* **1980**, *34*, 407−408.
(14) Vidrine, D. W. *Appl. Spectrosc.* **1980**, *34*, 314−319.
(15) Sampaolo, A.; Patimisco, P.; Giglio, M.; Zifarelli, A.; Wu, H.; Dong, L.; Spagnolo, V. *Anal. Chim. Acta* **2022**, *1202*, No. 338894.
(16) Dumitras, D. C.; Petrus, M.; Bratu, A. M.; Popa, C. *Molecules* **2020**, *25*, No. 1728, DOI: 10.3390/molecules25071728.
(17) Thakur, S. N.; Rai, V. N.; Singh, J. P. Chapter 3 - Physics and Techniques of Photoacoustic Spectroscopy of Liquids. In *Photoacoustic and Photothermal Spectroscopy*; Thakur, S. N.; Rai, V. N.; Singh, J. P., Eds.; Elsevier, 2023; pp 51−68.
(18) McGovern, S. J.; Royce, B. S. H.; Benziger, J. B. *Appl. Surf. Sci.* **1984**, *18*, 401−413.

(19) Ohtani, B. Photoacoustic Spectroscopy. In *Springer Handbook of Inorganic Photochemistry*; Bahnemann, D.; Patrocinio, A. O. T., Eds.; Springer: Cham, 2022.
(20) Low, M. J. D.; Parodi, G. A. *Spectrosc. Lett.* **1980**, *13*, 663−669.
(21) Riseman, S. M.; Eyring, E. M. *Spectrosc. Lett.* **1981**, *14*, 163−185.
(22) Low, M. J. D. *Spectrosc. Lett.* **1983**, *16*, 913−922.
(23) Rockley, M. G.; Ratcliffe, A. E.; Davis, D. M.; Woodard, M. K. *Appl. Spectrosc.* **1984**, *38*, 553−556.
(24) Low, M. J. D. *Spectrosc. Lett.* **1985**, *18*, 619−625.
(25) Carter, R. O., III; Paputa Peck, M. C.; Bauer, D. R. *Polym. Degrad. Stab.* **1989**, *23*, 121−134, DOI: 10.1016/0141-3910(89)90083-9.
(26) Ando, T.; Inoue, S.; Ishii, M.; Kamo, M.; Sato, Y.; Yamada, O.; Nakano, T. *J. Chem. Soc. Faraday Trans.* **1993**, *89*, 749−751.
(27) Yang, C. Q.; Simms, J. R. *Fuel* **1995**, *74*, 543−548.
(28) Saab, A. P.; Laub, M.; Srdanov, V. I.; Stucky, G. D. *Adv. Mater.* **1998**, *10*, 462−465.
(29) Obraztsov, A. N.; Pavlovskii, I. Y.; Okushi, H.; Watanabe, H. *Phys. Solid State* **1997**, *39*, 1594−1598.
(30) Pan, S.-W.; Lu, H.-C.; Lo, J.-I.; Ho, L.-I.; Tseng, T.-R.; Ho, M.-L.; Cheng, B.-M. *Sensors* **2022**, *22*, No. 3638, DOI: 10.3390/s22103638.
(31) Lo, J.-I.; Lu, H.-C.; Peng, Y.-C.; Chou, S.-L.; Cheng, B.-M. *Mon. Not. R. Astron. Soc.* **2021**, *508*, 1056−1063, DOI: 10.1093/mnras/stab2475.
(32) Lu, H.-C.; Cheng, B.-M. *Anal. Chem.* **2011**, *83*, 6539−6544.
(33) Chase, B.; Herron, N.; Holler, E. *J. Phys. Chem. A* **1992**, *96*, 4262−4266.
(34) Wang, K.-A.; Rao, A. M.; Eklund, P. C.; Dresselhaus, M. S.; Dresselhaus, G. *Phys. Rev. B* **1993**, *48*, 11375−11380.
(35) Martin, M. C.; Du, X.; Kwon, J.; Mihaly, L. *Phys. Rev. B* **1994**, *50*, 173−183.
(36) Homes, C. C.; Horoyski, P. J.; Thewalt, M. L. W.; Clayman, B. P.; Anthony, T. R. *Phys. Rev. B* **1995**, *52*, 16892−16900.
(37) Kuzmany, H.; Winkler, R.; Pichler, T. *J. Phys.: Condens. Matter* **1995**, *7*, 6601−6624.
(38) Guldi, D. M.; Prato, M. *Acc. Chem. Res.* **2000**, *33*, 695−703.
(39) Schettino, V.; Pagliai, M.; Ciabini, L.; Cardini, G. *J. Phys. Chem. A* **2001**, *105*, 11192−11196.
(40) Lu, H.-C.; Lin, M.-Y.; Peng, Y.-C.; Chou, S.-L.; Lo, J.-I.; Cheng, B.-M. *Mon. Not. R. Astron. Soc.* **2015**, *452*, 2788−2793, DOI: 10.1093/mnras/stv1460.
(41) Bethune, D. S.; Meijer, G.; Tang, W. C.; Rosen, H. J.; Golden, W. G.; Seki, H.; Brown, C. A.; de Vries, M. S. *Chem. Phys. Lett.* **1991**, *179*, 181−186.
(42) Xiang, Q.; Liu, Y.; Zhang, X.; Duan, Y.; Bumaliya, A.; Xiang, M. *J. Cluster Sci.* **2020**, *31*, 951−960.
(43) Sun, G.; Kertesz, M. *J. Phys. Chem. A* **2002**, *106*, 6381−6386.
(44) Nemes, L.; Ram, R. S.; Bemath, P. F.; Tinker, F. A.; Zumwalt, M. C.; Lamb, L. D.; Huffman, D. R. *Chem. Phys. Lett.* **1994**, *218*, 295−303.
(45) Jishi, R. A.; Dresselhaus, M. S.; Dresselhaus, G.; Wang, K.-A.; Zhou, P.; Rao, A. M.; Eklund, P. C. *Chem. Phys. Lett.* **1993**, *206*, 187−191.
(46) Davies, G. *Nature* **1981**, *290*, 40−41.
(47) Clark, C. D.; Davey, S. T. *J. Phys. C: Solid St. Phys.* **1984**, *17*, 1127−1140.
(48) Woods, G. S. *Proc. R. Soc. London, Ser. A* **1986**, *407*, 219−238.
(49) Ferrer, N.; Nogués-Carulla, J. M. *Diamond Relat. Mater.* **1996**, *5*, 598−602.
(50) Hill, H. G. M.; D'hendecourt, L. B.; Perron, C.; Jones, A. P. *Meteorit. Planet. Sci.* **1997**, *32*, 713−718.
(51) Linares, R.; Doering, P. *Diamond Relat. Mater.* **1999**, *8*, 909−915.
(52) Kaminsky, F. V.; Khachatryan, G. K. *Can. Mineral.* **2001**, *39*, 1733−1745.
(53) Iakoubovskii, K.; Adriaenssens, G. J. *Diamond Relat. Mater.* **2002**, *11*, 125−131.
(54) Lu, H.-C.; Lin, M.-Y.; Chou, S.-L.; Peng, Y.-C.; Lo, J.-I.; Cheng, B.-M. *Anal. Chem.* **2012**, *84*, 9596−9600, DOI: 10.1021/ac302545u.
(55) Davies, G.; Collins, A. T.; Spear, P. *Solid State Commun.* **1984**, *49*, 433−436.
(56) Rondeau, B.; Fritsch, E.; Guiraud, M.; Chalain, J.-P.; Notari, F. *Diamond Relat. Mater.* **2004**, *13*, 1658−1673.
(57) Lu, H.-C.; Lin, M.-Y.; Peng, Y.-C.; Lo, J.-I.; Chou, S.-L.; Cheng, B.-M. *Anal. Chem.* **2014**, *86*, 10497−10500.
(58) Lu, H.-C.; Peng, Y.-C.; Lin, M.-Y.; Chou, S.-L.; Lo, J.-I.; Cheng, B.-M. *Anal. Chem.* **2015**, *87*, 7340−7344.
(59) Novoselov, K. S.; Geim, A. K.; Morozov, S. V.; Jiang, D.; Zhang, Y.; Dubonos, S. V.; Grigorieva, I. V.; Firsov, A. A. *Science* **2004**, *306*, 666−669.
(60) Dresselhaus, M. S.; Jorio, A.; Souza Filho, A. G.; Saito, R. *Philos. Trans. R. Soc., A* **2010**, *368*, 5355−5377.
(61) Pumera, M.; Wong, C. H. A. *Chem. Soc. Rev.* **2013**, *42*, 5987−5995.
(62) Sahin, H.; Leenaerts, O.; Singh, S. K.; Peeters, F. M. *WIREs Comput. Mol. Sci.* **2015**, *5*, 255−272.
(63) Araujo, P. T.; Terrones, M.; Dresselhaus, M. S. *Mater. Today* **2012**, *15*, 98−109.
(64) Zhang, C.; Dabbs, D. M.; Liu, L. M.; Aksay, I. A.; Car, R.; Selloni, A. *J. Phys. Chem. C* **2015**, *119*, 18167−18176.
(65) Lin, Y.; Plaza-Rivera, C. O.; Hu, L.; Connell, J. W. *Acc. Chem. Res.* **2022**, *55*, 3020−3031.
(66) Abdolhosseinzadeh, S.; Asgharzadeh, H.; Kim, H. S. *Sci. Rep.* **2015**, *5*, No. 10160.
(67) Xu, Y.; Lin, Z.; Zhong, X.; Huang, X.; Weiss, N. O.; Huang, Y.; Duan, X. *Nat. Commun.* **2014**, *5*, No. 4554.
(68) Huang, J.-B.; Patra, J.; Lin, M.-H.; Ger, M.-D.; Liu, Y.-M.; Pu, N.-W.; Hsieh, C.-T.; Youh, M.-J.; Don, Q.-F.; Chang, J.-K. *Polymers* **2020**, *12*, No. 765, DOI: 10.3390/polym12040765.
(69) Dresselhaus, M. S.; Dresselhaus, G.; Saito, R.; Jorio, A. *Phys. Rep.* **2005**, *409*, 47−99.
(70) Costa, S.; Borowiak-Palen, E.; Kruszynska, M.; Bachmatiuk, A.; Kalenczuk, R. J. *Mater. Sci.* **2008**, *26*, 433−441, DOI: 10.1016/j.msec.2019.02.027.
(71) Bokobza, L.; Zhang, J. *eXPRESS Polym. Lett.* **2012**, *6*, 601−608.


https://doi.org/10.1021/acs.analchem.4c01797
*Anal. Chem.* 2024, 96, 10732−10737